

CO Hydrogenation on Nickel-Based Catalysts: Effects of Copper Addition

Miriam Agnelli¹ and Claude Mirodatos²

Institut de Recherches sur la Catalyse, 2 Avenue Albert Einstein, 69626 Villeurbanne Cedex, France

Received November 1, 1999; revised January 10, 2000; accepted January 17, 2000

The effect of copper addition on the catalytic properties of silica-supported nickel catalysts for the reaction of CO hydrogenation in the temperature range of 200–500°C has been investigated. Different effects, positive or negative, depending on the temperature and the copper content, are described and explained. At low temperature (230°C), the addition of a low copper content prevents the loss of the active surface by sintering without inhibiting the rate of CO hydrogenation too much. At high temperatures (450°C), high copper content is necessary to limit the accumulation of poisonous carbon products, but at the expense of CO conversion. On the basis of the various kinetic and morphologic effects of copper addition, an advanced description of the CO hydrogenation mechanism is also provided, assuming an active site formed by 2–3 adjacent Ni atoms, whatever the temperature or the copper content may be. © 2000

Academic Press

Key Words: catalytic CO hydrogenation; copper; nickel; mechanism.

INTRODUCTION

Within the renewed interest in the direct synthesis of hydrocarbons from syngas, the basic reaction of methanation can be considered either (i) as a target reaction for producing methane for further chemical use (including a recycling loop in reforming processes) or for burning as an auxiliary heat source or (ii) as a detrimental route when higher hydrocarbons and/or oxygenates are targeted such as those for the Fischer–Tropsch (FT) process or for methanol or higher alcohols syntheses (1). Whatever the process, advanced knowledge of the various parameters which control both activity/selectivity and catalyst aging is required. Nickel-based catalysts are generally considered as reference methanation catalysts, able to work efficiently in the temperature and pressure ranges of 200–500°C and 1000–7000 kPa (2). Deactivation processes remain, however, as the main drawback encountered for this reaction or its

reverse, the steam-reforming reaction. In the absence of chemical poisoning (by sulfide compounds or heavy metals), we demonstrated in previous works (3, 4) that the deactivation process can be considered a complex combination of particle sintering and carbon deposits, each factor depending on the reaction conditions. Thus, nickel sintering was shown to occur at rather low temperatures and high CO pressures by nickel carbonyl formation and transport and the process was fully modeled according to the initial nickel particle size distribution (3). Carbon deposition was shown to arise from the slow transformation of a nickel carbide overlayer into bulk carbide, followed by extra particle encapsulation and carbon poisoning. That process was also related to particle morphology since the formation of nickel carbide was found to be favored after particle sintering and smoothing (3, 4).

Apart from the tuning and optimizing of the operation conditions, the modification of the catalyst composition, such as by the addition of an inert element alloyed to nickel, can also be proposed as a way to limit the aforementioned deactivation processes. Note that a controlled inhibiting effect of methanation is also of interest when the C₁ route appears to be detrimental, as stated previously for FT synthesis. Copper was selected as such an additive because it does not easily dissociate CO, as is well established and reported in several reviews including the use of Ni–Cu alloys in CO hydrogenation (5–7). This low reactivity toward CO dissociation leads to the inhibition of CO activation on nickel–copper alloy due to dilution of the active nickel phase by the inactive copper atoms, in a way similar to that by other adatoms such as S, Hg or Sn (8). In addition, it was proposed that copper might inhibit the formation of carbonyl species involved in the nickel sintering process (9, 10). Thus, copper addition may lead to more stable but also to less active catalysts. For this reason, the global effect of catalyst promotion will be evaluated by catalyst activity and catalyst stability. The effect of copper addition on both deactivation processes of sintering and carbon deposition in the temperature range of 200–500°C, which corresponds to the thermodynamic domain where the onward methanation process dominates the backward reforming one, has been investigated.

¹ Present address: Centro de Investigación y Desarrollo en Criotecología de Alimentos, 47 y 116, (1900) La Plata, Argentina.

² Corresponding author: Fax: 04 72 44 53 99. E-mail: mirodato@catalyse.univ-lyon1.fr.

EXPERIMENTAL

Catalyst preparation. One Ni/SiO₂ and three NiCu/SiO₂ catalysts were prepared by impregnating (or co-impregnating) silica (Aerosil Degussa 200 m² g⁻¹) with nickel and copper nitrate hexamine solutions, according to (9, 11). The dried precursors were reduced *in situ* in flowing H₂ at 650°C for 15 h, the temperature being raised at 2°C min⁻¹. The nickel loading is 15 wt% for all the catalysts and the Cu/Ni atomic ratios are 0.03, 0.13, and 0.32 for the three copper-promoted ones.

CO hydrogenation. After activation, the catalyst was cooled down to reaction temperature in flowing H₂, and then the reaction mixture CO + 2H₂ was admitted into the reactor. The methanation reaction was carried out under differential conditions (conversions lower than 10%) at 230 and 450°C, after verification that no diffusion limitation occurred under such operating conditions. In reactions at high temperatures (450°C) the reaction mixture was diluted with He in a He/gaseous mixture at a ratio of 2.8. Catalytic runs were always started with a fresh catalyst. After variable times on stream (from 5 min to 90 h), the reactor was flushed with helium and cooled down to the required temperature for characterization.

Temperature-programmed hydrogenation (TPH). The used catalyst was heated from room temperature to 880°C in flowing H₂ at a heating rate of 8°C min⁻¹. The only detected product was methane and its concentration was followed continuously by gas chromatography and mass spectrometry.

Magnetic measurements. Magnetic measurements, based on the Weiss extraction method (12), were performed in an electromagnet, providing fields up to 21 kOe. From the value of the saturation magnetization, the degree of nickel reduction was determined, allowing verification of any possible loss of nickel during the reaction also. For nickel particles remaining in the superparamagnetic domain (diameter <15 nm), two average diameters of particles were determined: *D*₁ at high fields, corresponding to small particles, and *D*₂ at low fields, corresponding to large particles (13). This technique was also used to differentiate the various carbon species formed during methanation: (i) the species interacting chemically with metallic nickel (e.g., Ni₃C or interstitial carbon) causes a specific reduction of the magnetic signal since the nickel atoms involved in this interaction are no longer ferromagnetic; (ii) the noninteracting carbon species (e.g., whiskers, encapsulation graphite outside the particles) does not affect the overall ferromagnetic signal of the sample.

Electron microscopy. Fresh and aged samples were examined by transmission electron microscopy (TEM) to follow the evolution of the particle size distribution (PSD) with

time on stream when the reaction is carried out at different temperatures. This technique was also used for massive carbon accumulation detection.

Particle counting was done as explained in (3) from PSD and H₂ chemisorption data.

The composition of fresh and aged catalysts was analyzed by scanning transmission electron microscopy (STEM) combining electron micrographs with nanoanalysis by X-ray diffraction (EDX). Samples were prepared by making a suspension of the solid in a liquid medium using ultrasound. The dispersed particles were deposited on copper grids of 200 or 400 mesh and covered by a very thin film of carbon (<10 nm), allowing electron passage. Before observation, the grids were dried under infrared radiation (14).

Volumetric hydrogen chemisorption. Hydrogen chemisorption measurements were performed in conventional volumetric equipment. Equilibrium pressures were varied between 0 and 250 mbar. Before the isotherms were carried out, carbon residues on aged samples were eliminated under H₂ at reaction temperature. Then the samples were treated at 400°C for 1 h under vacuum to desorb H₂. From the amount of irreversibly adsorbed H₂, the metallic surface (i.e., the concentration of surface metal nickel atoms) was calculated, assuming a stoichiometry of H/Ni_S = 1 and a site density of 6.77 × 10⁻² nm²/atom (based on the assumption of an equal distribution of the three lowest index planes of nickel).

RESULTS

1. NiCu/SiO₂ Properties under Methanation at Low Temperature (230°C)

1.1. Changes in Catalytic Activity

The changes in specific catalytic activity (per catalyst weight unit) with time on stream at 230°C and atmospheric pressure are presented in Figs. 1A (normalized values) and 1B. The changes in initial activities (normalized by reference to the initial value of the nonpromoted Ni/SiO₂ catalyst) with copper content are reported in Fig. 2, curve a. Two effects of copper addition can be outlined:

(i) The initial activity is markedly decreased as the copper content is increased (Figs. 1B and 2a), as commonly reported by several authors (5, 7, 15).

(ii) Copper addition limits the deactivation rate (Fig. 1A). This effect tends to stabilize when the copper content increases. Inhibition on the deactivation rate may result from decreased catalyst activity with copper content. However, it can be noted that, after approximately 3 h of reaction, the activity of the Cu/Ni = 0.03 catalyst becomes higher than that corresponding to Ni/SiO₂ (Fig. 1B). Thus, the copper effect on the nickel deactivation rate cannot simply be assigned to a lower initial activity level.

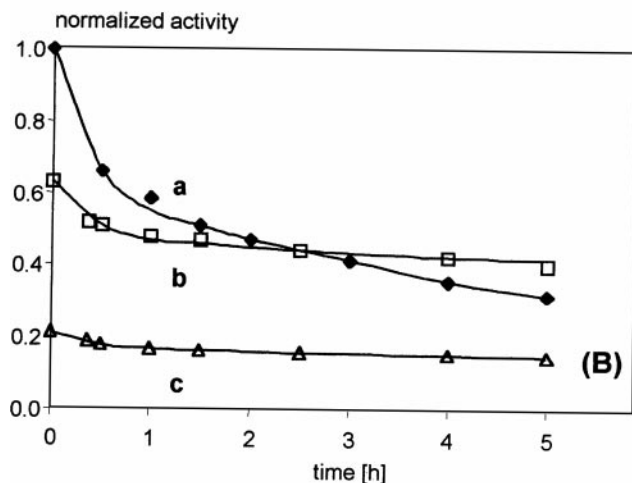
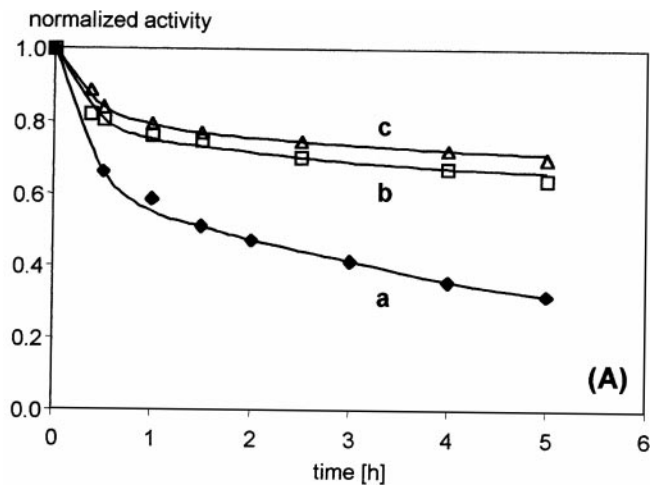


FIG. 1. NiCu/SiO₂ catalysts activity for CO/H₂ reaction at 230°C as a function of time on stream and copper content: (A) normalized with respect to each initial activity, (B) relative values, i.e., normalized with respect to the initial activity of the Ni/SiO₂ sample. Curves: (a) Cu/Ni = 0; (b) Cu/Ni = 0.03; (c) Cu/Ni = 0.13.

1.2. Carbon Deposits

TPH diagrams of NiCu/SiO₂ catalysts aged under CO/H₂ at 230°C present only one peak of methane formation with a maximum toward 200°C, like those for the nonpromoted catalyst. This carbon accumulation is quantified by calculating the atomic ratio of C/Ni_s with C deduced from TPH peak integration and Ni_s from the H₂ adsorption measurements after carbon elimination. As can be seen in Fig. 3, the C/Ni_s ratio increases with time on stream and stabilizes to 0.38 after about 3 h, independent of the copper content. In addition, the accumulating carbon species is found to interact chemically with the ferromagnetic (metal) nickel phase. Therefore, as was stated in (4, 16), this carbon species can be assigned to surface nickel carbide, Ni₃C, accumulating progressively upward to form a monolayer after around 3 h on a CO/H₂ stream.

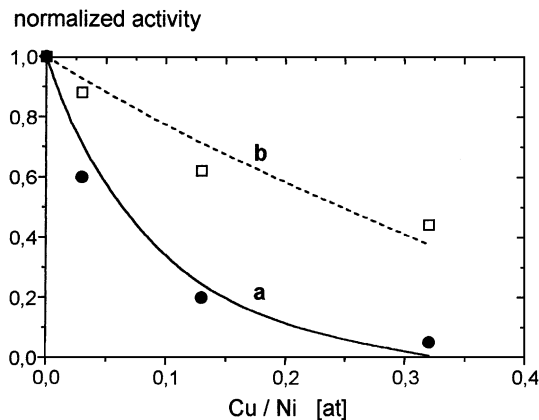


FIG. 2. Changes in initial catalytic activity of NiCu/SiO₂ catalysts with copper content under CO/H₂ reaction at 230°C (a) and 450°C (b). Full (230°C) and dotted (450°C) lines are the simulated curves obtained according to the ensemble model.

1.3. Sintering of the Metallic Active Phase

Magnetic measurements. The changes in particle size as a function of time on stream were followed by magnetic measurements as shown in Fig. 4. As was reported previously for the nonpromoted catalyst (3), all samples are characterized by a differentiated growth of particles: a fraction of the metal particles remains unchanged (D_1 in full line); meanwhile, another fraction increases its size with time on stream (D_2 in dashed line). In the case of NiCu catalysts, the initial particle diameter of the smallest particles, D_1 , tends to be higher than the one of the unpromoted sample. In addition, the mean particle diameter of the largest ones, D_2 ,

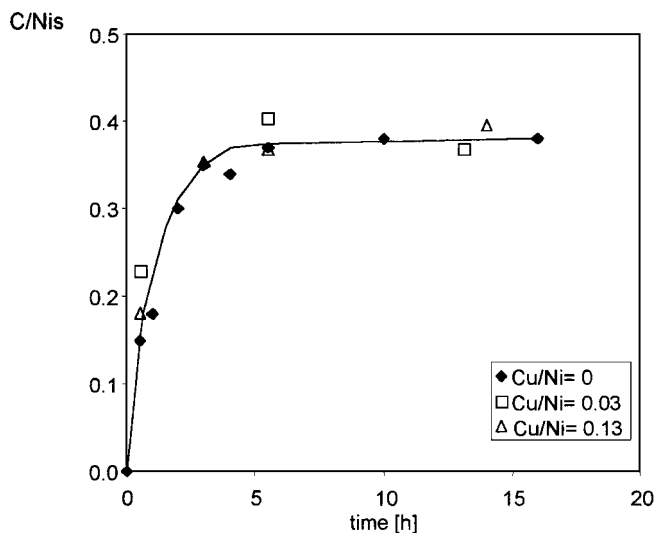


FIG. 3. Changes in the C/Ni_s ratio (atom of carbon per Ni surface atom) with time on stream for CO/H₂ reaction at 230°C on NiCu/SiO₂ catalysts.

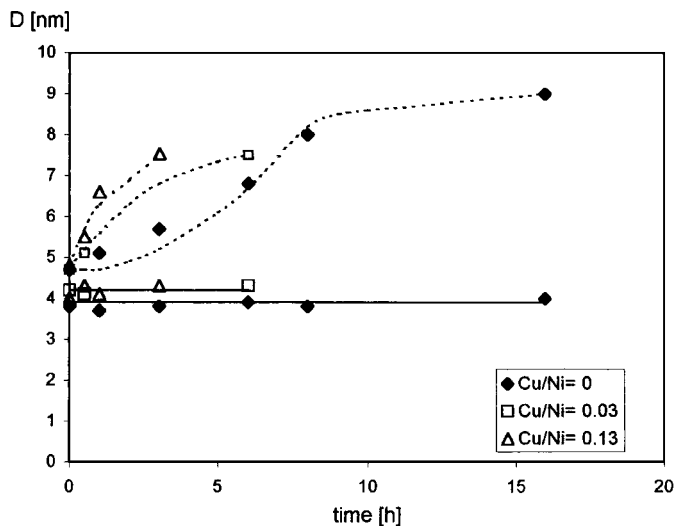


FIG. 4. Magnetic measurements: Changes in particle diameter (D_1 , in full line, and D_2 , in dashed line) of NiCu/SiO₂ catalysts with time on stream under CO/H₂ reaction at 230°C.

increases rapidly, and a remanent magnetization appears, indicating the presence of particles exceeding 15 nm. In a first approximation, it can be concluded that the rate of sintering is larger on Cu-promoted catalysts than on nonpromoted Ni/SiO₂. However, due to the appearance of magnetic remanence, the particle size cannot be established precisely by this technique.

Electron microscopy. Images of fresh and aged samples of the nonpromoted Ni/SiO₂ catalyst were reported in (3). Quite similar pictures were obtained for the bimetallic sample Cu/Ni = 0.13 treated under similar conditions. Initially, the particles are spherical and well dispersed on the support. After 3 h of reaction, a few faceted particles appear, and after 16 h, faceted particles are well developed in number and size, always coexisting with the small, spherical initial particles.

EDX nanoanalysis reveals that the particles of the fresh NiCu sample have a homogeneous chemical composition: the same Cu concentration (12.6 at.%) is obtained either for a single particle (high magnification) or for a group of particles (low magnification). These values also correspond to the ones obtained from chemical analysis (Table 1).

For the sample exposed to CO/H₂ reaction for 16 h the small particles display an increased copper content (16.5 at.%), while still keeping a homogeneous composition. In contrast, the large faceted particles contain nickel quasi-exclusively (Table 1). The mean residual concentration of copper (2.1 at.%) may be due effectively to the simultaneous analysis of small particles masked by the large ones. In any case, this confirms unambiguously that mass transfer during the sintering process occurs via nickel carbonyl, as copper does not form carbonyls under these conditions (3).

TABLE 1

Changes in EDX Analysis as a Function of Micrograph Enlargement and Time on a Methanation Stream at 230°C for the NiCu/SiO₂ Catalyst (Cu/Ni = 0.13)

Aging time at 230°C (h)	Overall Cu concentration ^a (at.%)	EDX Cu concentration ^b (at.%)	
		Small particles	Large particles
0	13.8	12.6	^c
16	13.2	16.5	2.1

^aDetermined by chemical analysis.

^bDetermined by EDX nanoanalysis.

^cNo large particles on fresh sample.

PSDs obtained from electron microscopy micrographs are shown in Fig. 5. Initially, the PSD is monomodal and narrow. After a few minutes of contact with CO/H₂ at 230°C, the PSD becomes broader and shifts toward higher values, still remaining monomodal. This means that some particles tend to decrease in size while others are expanding. After about 3 h on a methanation stream, some faceted particles appear, but so scarcely that PSD cannot be quantified until 5 h of aging has occurred. In contrast to the PSD of spherical particles, the PSD of the faceted ones is rapidly enlarged. Average particle sizes calculated from these distributions are reported in Table 2. These values are very close to those obtained for the monometallic catalyst Ni/SiO₂ for both types of particles.

Particle counting reveals that the number of spherical particles decreases with time on stream; meanwhile, the number of faceted ones remains constant. Besides, the number of small particles is higher for NiCu/SiO₂ than for the nonpromoted catalyst. In contrast, the number of the faceted particles is reduced by half.

These results show that the addition of copper effectively modifies the rate of faceting of the spherical particles. However, once the latter are formed, they grow very quickly.

TABLE 2

Changes in TEM Particle Mean Diameters as a Function of CO/H₂ Reaction Time at 230°C of Ni/SiO₂ and NiCu/SiO₂ Catalysts

Aging time on stream (h)	Ni/SiO ₂		NiCu/SiO ₂ (Cu/Ni = 0.13)	
	Small particles (nm)	Large particles (nm)	Small particles (nm)	Large particles (nm)
0	4.2	^a	3.8	^a
1	5.1	^a	5.1	^a
5	5.0	31.0	5.3	29.3
16	6.2	48.0	6.2	45.0

^aNo large particles.

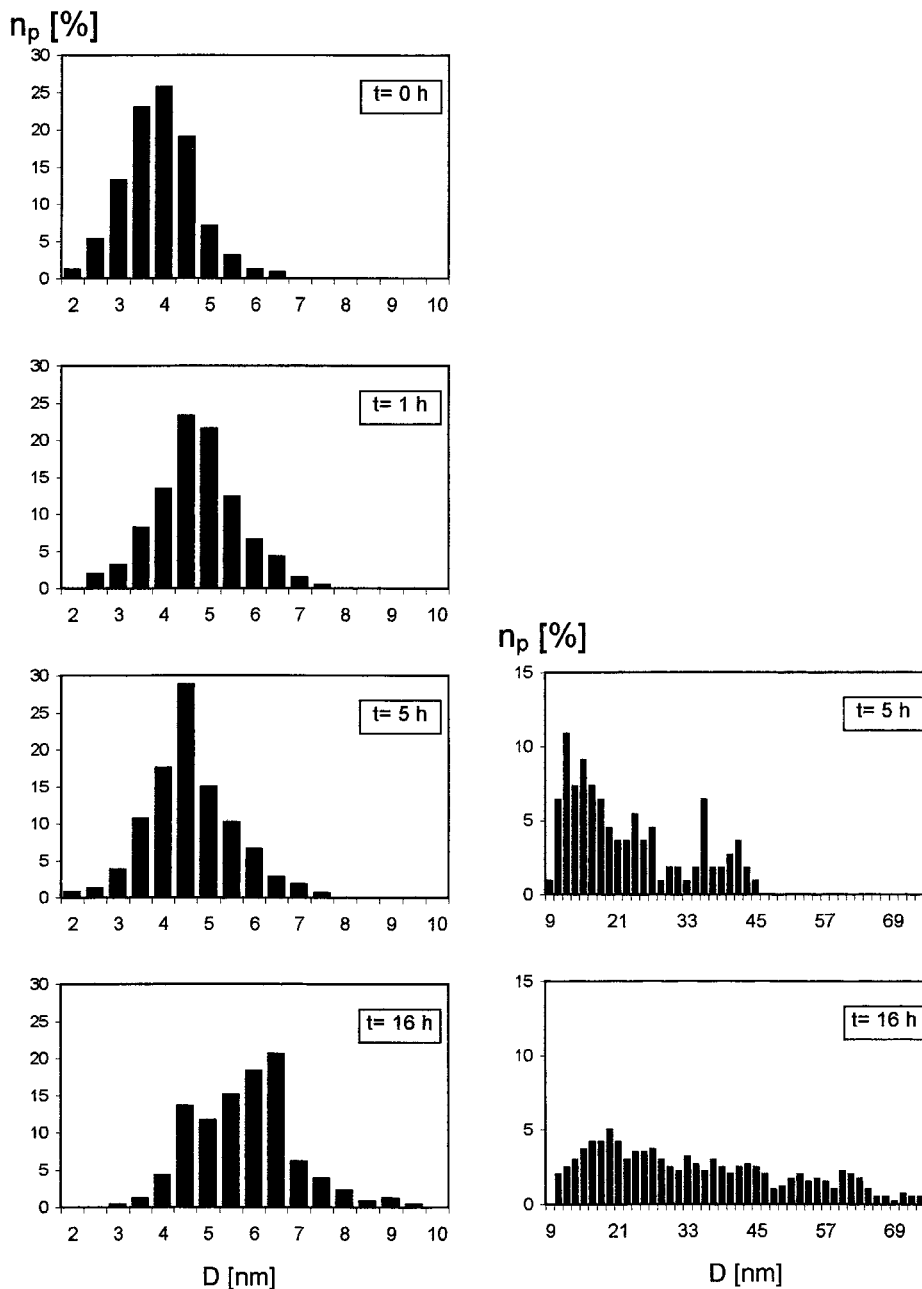


FIG. 5. Changes in particle size distribution of a NiCu/SiO₂ catalyst (Cu/Ni = 0.13) aged under CO/H₂ reaction at 230°C during different reaction times (0, 1, 5, and 16 h, respectively).

Changes in the metallic surface determined by hydrogen chemisorption. The metallic surface active in hydrogen chemisorption was measured by hydrogen chemisorption after various times on a methanation stream on surface-carbide-free samples (i.e., after carbon hydrogenation at reaction temperature). Figure 6 and Table 3 report the normalized and absolute values of the active surface for H₂ chemisorption as a function of the aging time for NiCu/SiO₂ and Ni/SiO₂ catalysts, respectively. The promoted sample with a copper content of Cu/Ni = 0.03 presents, after a few

TABLE 3

Changes in Active Metallic Surface (Measured by H₂ Chemisorption) of Ni/SiO₂ and NiCu/SiO₂ (Cu/Ni = 0.13) as a Function of Time on a CO/H₂ Stream at 230°C

Time on stream (h)	S (m ² g _{cat} ⁻¹)			
	0	1	5	16
Ni/SiO ₂	163.2	119.9	54.4	52.5
NiCu/SiO ₂	131.2	138.7	91.8	80.3

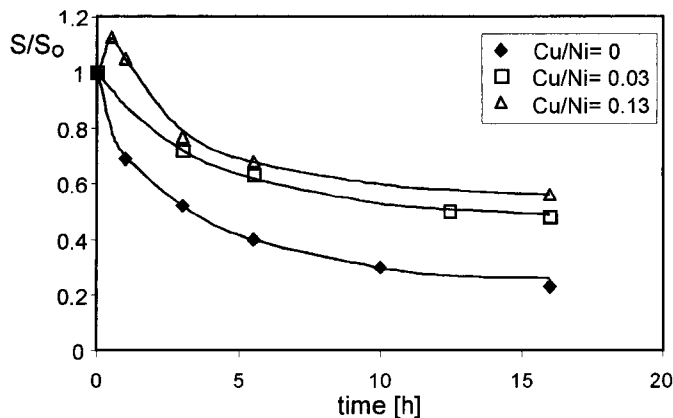


FIG. 6. Changes in metallic surface of Ni/SiO₂ and NiCu/SiO₂ catalysts with aging time, determined by H₂ chemisorption.

hours of reaction time, a higher metallic surface than that of the monometallic catalyst (Table 3). This explains why the promoted catalyst tends to have higher activity than that observed for the Ni/SiO₂ catalyst after a few hours of reaction (Fig. 1B). However, this positive result from copper addition stabilizing the active surface is overcompensated at a higher Cu content by the inhibiting effect on activity. Thus, for Cu/Ni = 0.13, the reaction should be carried out for a very long time to reach an activity level comparable to that of the Ni/SiO₂ catalyst (Fig. 1B, curve c). It was also observed that the copper-promoted samples presented during the very first period of reaction a transient increase of the nickel surface before a monotonic decay occurred. (See Fig. 6, for the case of the Cu/Ni = 0.13 sample. For the Cu/Ni = 0.03 sample, the metallic surface was not measured within this initial period.) The origin of that phenomenon will be discussed later. Note, however, that the transient increase in H₂ chemisorption in the initial period does not appear in the rate of methanation during the same period. This emphasizes the fact that the rate of methanation is not solely related to the metallic surface area able to chemisorb hydrogen.

2. NiCu/SiO₂ Properties under Methanation at High Temperature (450°C)

2.1. Catalytic Activity in CO Hydrogenation

The change in specific catalytic activity of NiCu/SiO₂ catalysts with time on stream for methanation reaction at high temperature is shown in Fig. 7 (normalized by reference to the initial value of each sample). As can be seen and in contrast to the effect found at low temperature (230°C), the relative loss of activity increases with copper content. As depicted in Fig. 2, the initial activity is much less copper-content-dependent at 450°C than at 230°C.

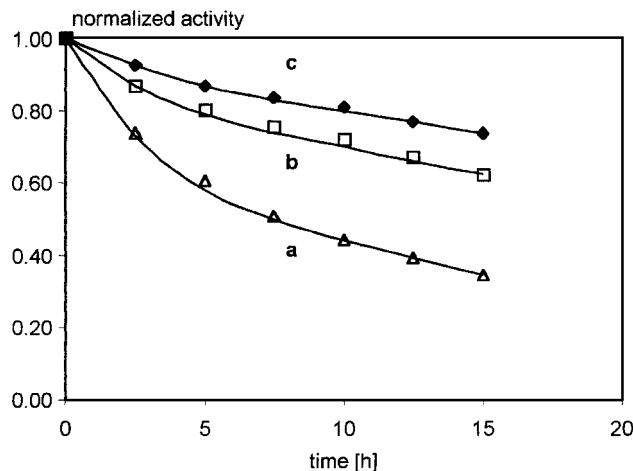


FIG. 7. Deactivation of NiCu/SiO₂ catalysts during CO/H₂ reaction at 450°C as a function of time on stream. Curves: (a) Cu/Ni = 0; (b) Cu/Ni = 0.03; (c) Cu/Ni = 0.13.

2.2. Carbon Deposition

Effect of time on stream. Figure 8 reports the TPH diagrams obtained for the nonpromoted Ni/SiO₂ sample reacted during increasing time on a CO/H₂ stream at 450°C. They reveal the presence of various types of carbon deposits:

- one form essentially hydrogenatable at low temperature ($T \cong 200^\circ\text{C}$);
- carbon species having intermediate reactivities toward hydrogen, forming a continuous background of methane production between 250 and 500°C;
- at least two forms of carbon deposits hydrogenatable above 500°C, with a slow production of methane still being observed at 900°C.

It can also be remarked that the temperature corresponding to the maximum of the peaks at high temperature shifts

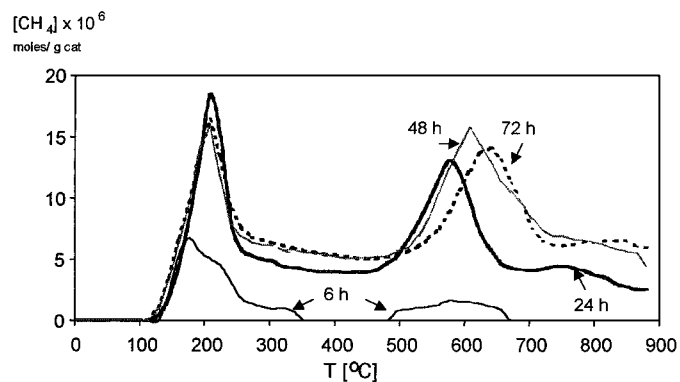


FIG. 8. Temperature-programmed hydrogenation diagrams of Ni/SiO₂ aged under CO/H₂ reaction at 450°C during different times on stream.

progressively to higher values with time on stream, indicating increasing stability of the species.

A precise deconvolution of such TPH diagrams is hazardous. Therefore, the analysis was simplified by considering only two types of carbon: one corresponding to the T range between ambient temperature and 400°C , referred to as C_{LT} (low-temperature carbon), and the other one corresponding to the T range between 400 and 900°C , referred to as C_{HT} (high-temperature carbon). Figure 9 shows that the amounts of C_{LT} and C_{HT} , reported as the atomic ratios C_x/Ni_s , increase with time on stream but in a different way:

(i) The $C_{\text{LT}}/\text{Ni}_s$ ratio increases regularly from 0 up to about 0.3 after 20 h of reaction and then practically stabilizes.

(ii) The C_2/Ni_s ratio remains negligible within an initial period when the C_{LT} species are developing and then starts to increase rapidly up to 20 h on stream. Afterward, it continues to grow at a slower rate. This trend suggests that C_{LT} species are primarily formed, while C_{HT} species are secondary by-products, formed from C_{LT} species.

TEM analysis of the aged samples did not evidence any form of vermicular or whisker-type carbon.

To define more precisely the nature of C_{LT} and C_{HT} deposits, magnetic measurements were carried out (a) on the activated fresh sample, (b) on the aged sample for 20 h under CO/H_2 reaction, (c) on the regenerated sample by carbon hydrogenation up to 400°C , and (d) after hydrogenation of most of the carbon deposits at 900°C . After 20 h of reaction (b), the magnetization of the sample decreases proportionally to the amount of deposited carbon with a stoichiometric ratio: deposited C/nonferromagnetic Ni ≈ 0.3 . After regeneration at 400°C (c) the initial magnetization is restored. After elimination of the high-temperature carbon (d), no further change in the ferromagnetic level is observed. These results reveal that

— C_{LT} presents the same characteristics as the monolayer of surface nickel carbide Ni_3C (nonferromagnetic) already

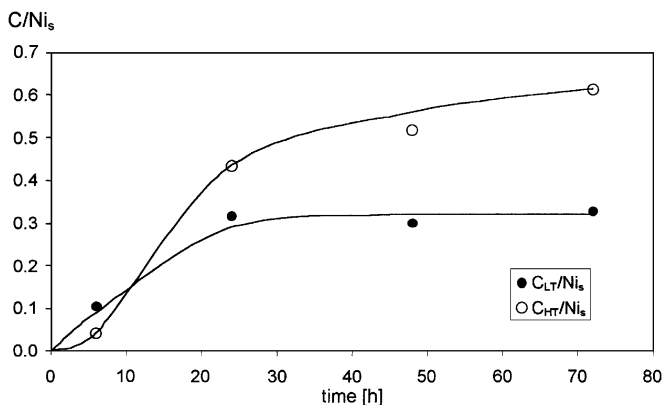


FIG. 9. Changes in $C_{\text{LT}}/\text{Ni}_s$ and $C_{\text{HT}}/\text{Ni}_s$ ratios with time on stream for CO/H_2 reaction at 450°C on Ni/SiO_2 catalyst.

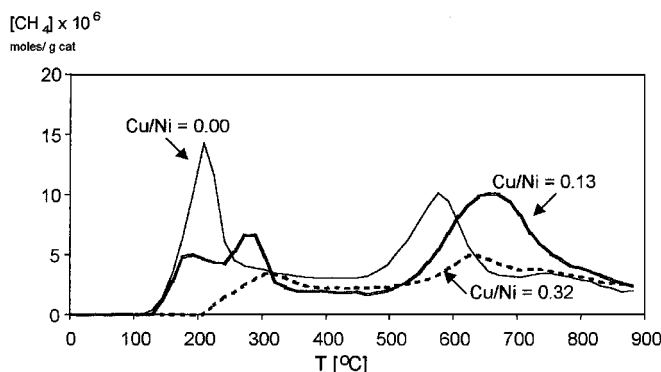


FIG. 10. Temperature-programmed hydrogenation diagrams of Ni/SiO_2 and NiCu/SiO_2 aged under CO/H_2 reaction at 450°C for 24 h.

identified during methanation at low temperature, though its accumulation is slower;

— C_{HT} is not chemically interacting with nickel, as it does not decrease the Ni particle ferromagnetism. It can be deduced that it is accumulated outside the particles. Its stability or extent of graphitization increases with time on stream.

Effect of copper addition. TPH diagrams of NiCu/SiO_2 catalysts (Fig. 10) show that the carbon species deposited during reaction at 450°C present a reactivity toward hydrogen which differs markedly from that observed for the monometallic catalyst:

(i) Copper addition provokes a progressive disappearance of the carbon form hydrogenatable at 200°C and the appearance of a second less reactive species hydrogenatable at 280°C . These two species coexist on the $\text{Cu}/\text{Ni} = 0.13$ catalyst. For higher contents ($\text{Cu}/\text{Ni} = 0.32$), the more reactive carbon form hydrogenatable at low temperature has practically disappeared. It must be noted, however, that the ratio of these two low-temperature species lumped together (i.e., C_{LT} species, according to the aforementioned nomenclature) to the surface nickel atom concentration remains constant, whatever the copper content may be, and equal to the value obtained for the monometallic catalyst, i.e., 0.3–0.4 (Fig. 11).

(ii) The TPH peaks related to the high-temperature carbon species (i.e., C_{HT} species) are shifted to higher temperatures. The $C_{\text{HT}}/\text{Ni}_s$ ratio increases regularly with copper content (Fig. 11) despite the fact that the absolute amount of carbon decreases as the Cu/Ni ratio increases.

2.3. Sintering of the Metallic Active Phase

The TEM and magnetic measurements for Ni/SiO_2 and NiCu/SiO_2 catalysts aged under CO/H_2 at 450°C showed that the average particle size remains constant with time on stream and equal to 4.0 nm. In addition, the size distribution remains monomodal.

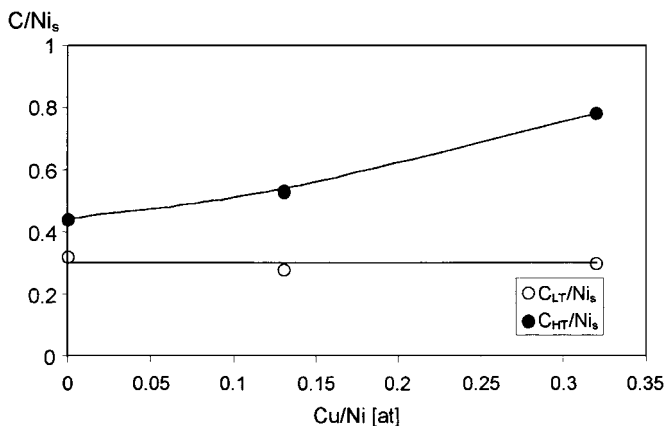


FIG. 11. Changes in C_{LT}/Ni_s and C_{HT}/Ni_s ratios on NiCu/SiO₂ catalysts aged under CO/H₂ reaction at 450°C for 24 h as a function of the Cu/Ni ratio.

DISCUSSION

Effect of Copper Addition under Low-Temperature Methanation Conditions

In the domain of low-temperature methanation, three main features related to copper addition were pointed out: (i) inhibition of the catalyst activity, (ii) stabilization of the active surface, and (iii) absence of effect on active carbon deposition.

(i) *Inhibition of the catalyst activity.* The nickel specific activity is strongly and not linearly inhibited upon copper addition, as revealed by the changes in initial activity versus copper content in Fig. 2. As already outlined in (5, 6, 11, 15), this inhibition effect is likely to come from a geometric effect of dilution of the active Ni phase by the inactive Cu phase. A model was proposed in (15) assuming that the nickel-specific activity A_x decreases as a function of the copper content x following the equation $A_x = A_0(1 - x)^w$, w being the number of adjacent Ni atoms involved in an active site for CO hydrogenation. Applying such an “ensemble model” to the present data leads to a rather large value of $w = 14 \pm 2$ as shown by the simulated curve a (solid line). In contrast, the size of the active hydrogenation site was found to be only 2 ± 1 adjacent Ni atoms for the non-promoted Ni/SiO₂ after a thorough kinetic study carried out by isotopic transient kinetics (4, 16). The size of the active site was directly related to the surface occupancy of the most abundant reacting intermediate (CH) leading to methane formation (16).

There is therefore a major discrepancy between the size of the active site found for the monometallic sample ($w = \sim 2$ Ni atoms) and the much larger size found for the case of a bimetallic surface ($w = \sim 14$ atoms). A first explanation could be that the geometric dilution effect of copper would be reinforced by an electronic effect such

as a short-distance electron transfer between Ni and Cu, which would deactivate the Ni atoms surrounding the copper ones (15). Another explanation is to stress that, under low-temperature methanation conditions, one *cannot* consider the whole catalyst a homogeneous alloy. As a matter of fact, and this will be discussed later in detail, even at short contact times and before the appearance of large faceted nickel particles, the fast carbonylation process selectively extracts nickel from the small particles and then increases the particles concentration into copper as compared to the overall Cu content of the sample. This means that the dilution effect observed in Fig. 2a should be modeled according to a much larger concentration of copper, which would substantially decrease the overestimated value of w . The latter explanation will be privileged after the copper effect at high temperature is considered.

(ii) *Stabilization of the active surface.* During the methanation reaction at low temperature, the addition of copper to Ni/SiO₂ was also shown to stabilize the active surface essentially by limiting the rate of particle sintering. This stabilizing effect is essentially visible for low copper contents (Fig. 1B, curve b). Thus, the nonpromoted catalyst Ni/SiO₂, which displays the highest initial activity, becomes less active than the weakly promoted one (Cu/Ni = 0.03) after a few hours of aging. At higher copper content (Cu/Ni \geq 0.13), the initial activity is so reduced that the stabilizing effect of copper is masked. This points out the existence of an optimum copper content, which corresponds to values around Cu/Ni = 0.03.

The question arises now of the origin of the nickel-sintering inhibition upon copper addition.

STEM analysis has demonstrated that nickel is selectively extracted from the bimetallic particles to form large faceted crystals; meanwhile, the small particles are progressively surface-enriched into copper. This process of nickel transport via surface carbonyls implies the transient formation of a highly dispersed nickel phase arising from the extraction of metal from the initial alloy and its recondensation into very small Ni particles, precursors of the large ones. The transient existence of very small nickel particles is revealed by the transient increase of the active surface (measured by H₂ chemisorption) within the first hour on stream, as shown in Fig. 6 for the Cu/Ni = 0.13 sample.

Thus, the sintering of NiCu catalysts presents the same main characteristics as those encountered for Ni/SiO₂: nickel atoms migrate as carbonyl or subcarbonyl species from the initial small bimetallic particles to recondense as large faceted particles of pure nickel during the reaction. Note that this simplified scheme does not exclude the fact that carbonyl species also form on large particles, but here the probability of recombining on the same particle is very high, which would explain the observed faceting of these large particles. In contrast, with the small particles, the Ni(CO)_{*n*} interacts as soon as it has formed with the support

and migrates until it meets another particle to decompose. However, specific features due to the presence of copper have been identified: if the PSD and average size particle changes are analogous for NiCu/SiO₂ (Ni/Cu = 0.13) and for Ni/SiO₂ with time on stream, the number of large particles formed during the reaction is decreased by half for the former. In addition, the number of small spherical particles decreases at a slower rate, resulting in a slower loss of active surface for the bimetallic catalysts.

From the aforementioned observations, the decrease of the sintering rate found on bimetallic particles can be ascribed to the effect of inhibition by copper on the rate of formation of nickel subcarbonyl species. In contrast, the steps of carbonyl species migration on the support or their recombination on the faceted crystals should not be affected by the presence of copper.

We have already proposed in (3) that the formation of subcarbonyl species (NiCO, Ni(CO)₂, and Ni(CO)₃) is favored on Ni atoms located at corners, edges, and other defects, that is, presenting an incomplete coordination. In the case of alloy particles, copper is likely to occupy preferentially surface defects, for thermodynamic reasons, which would induce a certain surface smoothing. This hypothesis is consistent with the fact already reported in the literature that adding copper to nickel limits both the multibonding adsorption of CO (dilution effect) and the formation of subcarbonyl species (smoothing effect), favoring the linear Ni-CO adsorption mode (5, 6, 13, 14). This trend may therefore explain the resistance of NiCu particles to carbonylation, though other side effects of copper cannot be discarded.

Thus, the mechanism of NiCu sintering can be described by the same model as the one proposed for Ni/SiO₂ in (3), differing only by surface reactivity parameters. This model, based on a modified "Ostwald ripening" process, assumes that the concentration of large particles is determined from the concentration of monomeric nickel carbonyl species. Since the evaporation rate (i.e., the rate of nickel extraction by carbonylation) is inhibited in the case of the bimetallic catalyst, the monomer concentration will be lower and the number of faceted particles formed from them will diminish too. In contrast, the condensation rate on faceted particles will be the same as that observed for the monometallic catalyst since it depends only on the morphological parameters (shape, surface tension) of the large pure nickel particles. So, as far as size is concerned, the faceted particles should present the same kinetic evolution for a monometallic and bimetallic catalyst. All these model predictions are perfectly confirmed experimentally.

(iii) *Active carbon deposition.* As unambiguously revealed in Fig. 3, the addition of copper does not modify the process of active surface carbidization when methanation is carried out at 230°C since the same ratio of 0.38

carbon atoms per surface nickel atom is found after a few hours of reaction on both nonpromoted and promoted catalysts.

From a mechanistic point of view, the formation of surface carbide during methanation at low temperature was shown to result from the dissociation of CO into surface oxygen and carbon (also called C_α, as proposed by several authors who established a recognized nomenclature of the various forms of carbon deposits arising from CO hydrogenation over various metals such as Ru or Ni (4, 16, 19–21)). That surface carbon may then be hydrogenated progressively into CH_x adspecies to further desorb as methane. The rate-determining step (RDS) was shown in (4, 16) to be the hydrogenation of accumulated carbide species into CH₂ intermediates and the concentration of active sites for that hydrogenation step was shown to be kinetically controlled by the surface coverage by linear CO (16). Thus, under steady-state conditions, the carbide layer is stable. As a matter of fact, as soon as a surface carbon atom is hydrogenated into CH₂ and thereafter rapidly into methane, an adsorbed CO species immediately decomposes into surface oxygen (which may easily react with activated hydrogen directly into water or into surface hydroxyl decomposing into water) and into surface carbon, reconstituting the adlayer. It may be stressed here that the fact that the buildup of a carbide layer is copper-independent does not contradict the well-established statement that CO dissociation is hindered upon Cu addition (5–8). This simply indicates that the RDS for methanation is not related to CO dissociation but to the additional steps of CH_x hydrogenation, as recalled previously.

Before that steady-state turnover of the catalytic cycle is reached, an initial period of about 3 h is required for building up the carbidic monolayer starting from the fresh sample during methanation at low temperature (Fig. 3). Due to the perfect coincidence between that time constant and the one corresponding to the particle sintering and smoothing process (3–5 h are required for the appearance of the large faceted particles, Fig. 5), both processes are most likely closely related. A very plausible explanation for that relationship is the following:

The formation of surface carbide was shown to be enhanced on dense (111) planes on single crystals, due to a better local structure (C_{3v} symmetry) for carbon stabilization (22). Since the faceted particles formed after about 3 h present a prominent (111) surface orientation (3), this explains why surface carbide formation and particle sintering/faceting coincide.

In addition, the kinetic process which controls large particle formation (nickel carbonyl condensation) and faceting was shown to be independent of the copper content (in both cases it concerns pure nickel particles). Observation that the kinetics of nickel carbide buildup is also copper-content-independent (Fig. 3) reinforces the previous statement that both processes are closely linked.

Effect of Copper Addition under High-Temperature (450°C) Methanation Conditions

The addition of copper to a Ni/SiO₂ catalyst leads to three major effects when the methanation is carried out at high temperature (450°C): (i) the decrease in the catalyst's initial activity (Fig. 2), (ii) the formation of a similar carbide-like monolayer, and (iii) the increase of the deactivation rate (Fig. 7).

(i) *Decrease in the initial catalyst activity.* As depicted in Fig. 2, the initial activity is much less sensitive to copper content at 450°C (b) than at 230°C (a). When the same modeling procedure as that applied for low-temperature data is followed, the size of the active site at high temperature is found to be $w = 2.5 \pm 0.4$ Ni atoms, as determined from the simulated curve b (dotted line). This value is now quite consistent with the value determined by transient kinetics on the monometallic sample (4). We have shown that at 450°C no sintering process occurs under reaction conditions, due to the fact that the nickel carbonyl species is not stable at high temperature. This means that the discrepancy found at low temperature for the size of the active site (≈ 14 vs ≈ 2 adjacent Ni atoms) is effectively due to an underestimation of the copper concentration of the small particles (which represents the main part of the active surface) due to nickel carbonylation and sintering. Thus, a straightforward calculation based on the simple ensemble model used to simulate curves a and b in Fig. 2 indicates that the actual copper concentration of the small particles at 230°C is about four times the overall concentration measured by chemical analysis. In contrast, at high temperature (450°C), the Ni-Cu alloy remains homogeneous all along the reaction run, which allows the ensemble model to be applied correctly.

(ii) *Carbide-like monolayer formation.* When methanation is carried out at 450°C, the formation of a surface nickel carbide monolayer is still observed (Fig. 9, curve C_{LT}/Ni_S), independent of the copper content (Fig. 11, curve C_{LT}/Ni_S).

Let us consider the case of the monometallic sample Ni/SiO₂. When completed, the carbide phase presents the same stoichiometry (Ni₃C) and reactivity toward hydrogen as surface carbides found at low temperature (230°C). This result shows direct evidence that the capacity to accumulate carbon under methanation conditions is practically temperature-independent. That statement can even be extended to the high-temperature domain of methane steam or dry reformation (actually the reverse reactions of methanation between 600 and 800°C) for which a similar buildup of surface carbide was found on close Ni/SiO₂ catalysts (23, 24).

The only difference between high- and low-temperature methanation lies in the fact that the rate of formation of this carbidic phase is much slower at high temperature

(completion within 3 and 20 h at 230 and 450°C, respectively).

Since at 450°C no sintering effect occurs during methanation runs, the kinetics of carbide layer buildup have to be controlled by other factors. Under these high-temperature methanation conditions, the lower surface coverage with CO (directly observed by *in situ* DRIFT as reported in (16)) is expected to facilitate hydrogen activation since more free nickel sites are available. This will result in lower stability (or lifetime) of surface carbon and therefore explain the much longer time required to build up the carbide adlayer. In addition, at high temperature the carbide phase also contributes to the formation of more stable carbon species by slow graphitization (Figs. 8 and 9), which may also slow down the completion of the adlayer.

A second important question which concerns the carbide-like monolayer buildup at 450°C is its copper content dependency. If one considers all the carbon species which can be hydrogenated at low temperature in TPH spectra (C_{LT} below 400°C in Fig. 10), the formation of the carbide-like monolayer appears to be independent of the copper content, at least for the low Cu content range investigated (Fig. 11, curve C_{LT}/Ni_S). This points out that the alloying effect of nickel by copper does not affect the amount of carbon insertion into the nickel phase. However, it was shown on the same TPH spectra that the species most reactive toward hydrogen (around 200°C) was progressively replaced by less reactive species hydrogenated at 280°C as the quantity of added copper increased.

The reactivity of this latter species corresponds to the reactivity generally observed for a form of bulk carbide which could be referred to as C_β or C_γ following the usual literature nomenclature (20, 21). Despite the fact that bulk carbide by itself is not toxic for the methanation reaction (unless under reforming conditions when it promotes whiskers formation and particle fragmentation (23, 24)), it reveals evolution of surface reactivity sensitive to copper addition. A combined geometric and electronic effect of the copper addition diluting the nickel phase could account for these changes in the nature and reactivity of the carbide-like adlayer.

(iii) *Deactivating carbon deposition.* TPH spectra revealed that, in addition to reactive carbon deposition (C_α and C_γ), a second type of carbon is accumulating progressively with time on stream (Fig. 9, curve C_{HT}/Ni_S) and proportionally to the copper content (Fig. 11, curve C_{HT}/Ni_S). These species were shown by TEM not to be vermicular carbon and by magnetic measurements not to interact chemically with the nickel phase. The observation of progressive catalyst deactivation simultaneous with this carbon accumulation strongly suggests that this form of toxic carbon encapsulates the Ni particles and therefore limits the available active surface. This type of encapsulating carbon, also observed under given reforming conditions at higher

temperatures (600–800°C) (24), is most likely due to the two-dimensional polymerization of surface carbide species around the metal particles.

Since in this domain of high-temperature methanation deactivation is only due to the formation of encapsulating carbon around the surface, the negative effect of copper on the deactivation rate could be related to higher stability of these species formed during the reaction (i.e., a higher degree of polymerization hindering the access of the reactants to the active surface). Effectively, it was observed by TPH that the reactivity toward hydrogen of the most stable carbon species decreases with copper addition, in a way similar to that seen for the less stable species discussed previously (Fig. 10).

The origin of surface, bulk, or external carbon species may be considered the result of competition between the hydrogenation of the monomeric C_α arising from CO dissociation into methane and its transformation into surface carbide, then into bulk carbide, and then into polymerized species around the particles (4).

This competition between surface reactions was already revealed by the influence of the ratio H_2/CO . Gardner and Bartholomew (25) reported the absence of vermicular carbon during methanation in the temperature range 350–450°C on a Ni/Al_2O_3 catalyst when the H_2/CO ratio was varied between 0.5 and 3. In contrast, when this ratio was lower than 0.25, a multiple layer of carbon appeared in a few minutes.

In the present case, the hydrogen activation capacity of $NiCu/SiO_2$ catalysts decreases proportionally as the Cu/Ni ratio increases (Fig. 6). This results in stabilization of surface carbide (longer lifetime), favoring its transformation via bulk carbide into more stable (therefore more deactivating) encapsulating external carbon film.

CONCLUSION

The addition of copper to a Ni/SiO_2 catalyst leads to different effects, positive or negative, depending on the temperature range and on the copper content:

—At low temperature (230°C), the main factor of deactivation is the sintering of the nickel active phase via carbonyl formation/transport/decomposition. Among the several effects of copper addition already well documented in the literature such as the inhibition of CO activation, the paper outlines the inhibition effect of copper on nickel carbonylation. However, low copper contents are required for obtaining a positive effect, i.e., preventing sintering without inhibiting the rate of CO hydrogenation too much.

—At high temperature (450°C), the main deactivation phenomenon is the formation of stable carbon deposits encapsulating the metal particles. The addition of copper contributes to the formation of less but more stable species by reducing the hydrogenating capacity of the nickel phase. High contents of copper are thus necessary to limit the accumulation of carbon products, toxic or not, but at the

expense of the CO conversion. The overall effect of copper for these conditions can be considered negative unless a reduction of the methanation capacity is targeted.

With analysis of the effect of copper addition on activity at different temperatures, it was deduced that the active site for CO hydrogenation is an ensemble of 2–3 adjacent Ni atoms, regardless of temperature or copper content. Certain literature discrepancies on that subject can be explained by considering that at low temperature the active phase (essentially the small particles) is enriched into copper (about 4 times the bulk composition) due to selective nickel extraction via carbonylation.

REFERENCES

- Saint-Just, J., Bousquet, J. M., and Martin, G. A., *La Recherche* **21**, 222 (1990).
- Vannice, M. A., *Catal. Rev. Sci. Eng.* **14**, 153 (1976).
- Agnelli, M., Kolb, M., and Mirodatos, C., *J. Catal.* **148**, 9 (1994).
- Agnelli, M., Swaan, H. M., Marquez-Alvarez, C. H., Martin, G. A., and Mirodatos, C., *J. Catal.* **117**, 117–128 (1998).
- Ponec, V., in "New Trends in CO Activation" (L. Guzzi, Ed.), Studies in Surface Science and Catalysis, Vol. 64, p. 117. Elsevier, New York, 1991.
- Schwanck, J., in "New Trends in CO Activation" (L. Guzzi, Ed.), Studies in Surface Science and Catalysis, Vol. 64, p. 225. Elsevier, **64**, 225 (1991).
- Ponec, V., and Bond, G. C., in "Catalysis by Metals and Alloys," Studies in Surface Science and Catalysis, Vol. 95. Elsevier Science BV, Amsterdam, 1995.
- Millians, D. E., Pritchard, J., and Sykes, K. W., in "Proceedings, 6th International Congress on Catalysis, London 1976" (G. C. Bond, P. B. Wells, and F. C. Tompkins, Eds.), Vol. 1, p. 417. The Chemical Society, London, 1977.
- Brum Pereira, E., and Martin, G. A., *Appl. Catal.* **103**, 291 (1993).
- Soma-Noto, Y., and Sachtler, W. M. H., *J. Catal.* **34**, 162 (1974).
- Dalmon, J. A., *J. Catal.* **60**, 325 (1979).
- Selwood, P. W., "Chemisorption and Magnetization." Academic Press, New York, 1975.
- Primet, M., Dalmon, J. A., and Martin, G. A., *J. Catal.* **46**, 25 (1977).
- Gallezot, P., and Leclerc, C., in "Catalyst Characterization, Physical Techniques for Solid Materials," (B. Imelik and J. C. Vedrine, Eds.), p. 509. Plenum, New York, 1994.
- Dalmon, J. A., and Martin, G. A., in "Proceedings, 7th International Congress on Catalysis, Tokyo, 1980" (T. Seiyama and K. Tanabe, Eds.), p. 409. Elsevier, Amsterdam, 1981.
- Márquez-Alvarez, C., Martin, G. A., and Mirodatos, C., in "Natural Gas Conversion V" (A. Parmaliana *et al.*, Eds.), Studies in Surface Science and Catalysis, Vol. 119, p. 155. Elsevier, Amsterdam, 1998.
- Dalmon, J. A., Primet, M., Martin, G. A., and Imelik, B., *Surf. Sci.* **59**, 45 (1975).
- van Dijk, W. L., Groenewegen, J. A., and Ponec, V., *J. Catal.* **45**, 277 (1976).
- Gupta, N. M., Kamble, V. S., Annaji Rao, K., and Iyer, R. M., *J. Catal.* **60**, 57 (1979).
- Winslow, P., and Bell, A. T., *J. Catal.* **86**, 158 (1984).
- Bartholomew, C. H., *Catal. Rev. Sci. Eng.* **24**, 67 (1982).
- Bertolini, J. C., and Imelik, B., *Surf. Sci.* **80**, 586 (1979).
- Swaan, H. M., Kroll, V. C. H., Martin, G. A., and Mirodatos, C., *Catal. Today* **21**, 571 (1994).
- Kroll, V. C. H., Swaan, H. M., and Mirodatos, C., *J. Catal.* **161**, 409 (1996).
- Gardner, D. C., and Bartholomew, C. H., *Ind. Eng. Chem. Process Res. Dev.* **20**, 80 (1981).